JOURNAL OF MATERIALS SCIENCE **26** (1991) 4808–4812

Electrical conductivity of zinc ferrites near stoichiometry and manganese–zinc ferrites under vacuum or in the presence of oxygen

B. GILLOT
Laboratoire de Recherches sur la réactivité des Solides UA 23, Faculté des Sciences Mirande, BP 138, 21004 Dijon Cedex, France

M. EL GUENDOUZI
Université Hassan II, Faculté des Sciences II, BP 6621, Casablanca, Morocco

P. PERRIAT
Thomson LCC, BP 18, 21201 Beaune Cedex, France

The electrical conductivity of zinc ferrites near stoichiometry and of manganese–zinc ferrites has been investigated as a function of temperature under vacuum and in the presence of oxygen. Under vacuum, the conductivity of these ferrites with iron excess is explained by the hopping mechanism, and with ZnO excess by the development of vacancies in octahedral sites of cation-deficient spinel. Activation energies and the transition temperatures are presented. During the oxidation in oxygen of Mn–Zn ferrites, the profile of the $\log \sigma = f(T)$ curves shows that the mechanism of electrical conduction in the temperature range 100 to 350 °C can be explained in terms of the oxidation of Fe^{2+} to Fe^{3+} ions at octahedral sites. For the temperature range 300 to 450 °C, the conductivity involves the hopping of electrons from octahedral sites of Mn^{3+} ions to octahedral sites of Mn^{4+} ions. Above 550 °C the oxidation of Mn^{2+} ions leads to a marked change in conductivity with the generation of new phases.

1. Introduction

The conduction of ferrites is usually described as a jumping of electrons between the ferrous ions and ferric ions on octahedral positions in the spinel lattice [1]. If ferrites contain manganese, the conductivity may also depend on the concentration, valency and distribution between the spinel tetrahedral and octahedral sublattices of manganese ions [2]. In addition, the complex oxido-reduction reactions involved during the rise of temperature prescribed by the sintering of Mn–Zn ferrites used as soft magnetic materials strongly determine their mechanical characteristics during the binder removal stage at low temperature (< 400 °C), as the mechanical strength has been found to be correlated with Fe^{2+} ion content and manganese oxidation state [3, 4].

In a previous paper [5] the oxidation–reduction mechanism of these Mn–Zn ferrites having an excess of iron, $Mn_xZn_yFe_{2.044}O_4$ with $x + y = 0.956$, has been investigated by thermogravimetry in order to establish a correlation between the thermal behaviour in oxygen and the cationic distribution. It has been shown that the marked preference of cations for certain sites (Fe^{2+} and Mn^{3+} ions for octahedral sites and Mn^{2+} and Zn^{2+} ions for tetrahedral sites) governs the reactivity, giving rise to distinct oxido-reduction phenomena as a function of temperature and oxygen partial pressure [6]. On the basis of this analysis it was found that below about 500 °C, these ferrites are oxidized in cation-deficient spinels but the oxidation depends highly on oxygen pressure. With increasing temperature, further oxidation of Mn^{2+} ions results in the appearance of α-Fe_2O_3 accompanied by a cation-deficient spinel.

In the present paper, results are reported on the electrical properties of several Mn–Zn ferrites and an attempt has been made to use the electrical conductivity to characterize the process of oxidation at temperatures up to 750 °C, and thus to relate the electrical behaviour with the oxidation degree of iron and manganese. Moreover, as the oxygen pressure in the atmosphere and the firing temperature determine zinc losses [7–9] which produce abrupt changes in conductivity as the stoichiometry varies from an iron deficiency to an iron excess, samples of zinc ferrites with a graduated zinc content have been investigated. The effect of preparation method on the electrical behaviour is also reported.

2. Samples and experimental procedure

Ferrite samples of composition $Mn_xZn_yFe_{2.044}O_4$ ($x + y = 0.956$) with $x = 0$, 0.25, 0.50, 0.70 and 0.956 were prepared by a standard ceramic route under air at 1200 °C. Details of the preparation were given in an

0022-2461/91 $03.00 + .12

earlier publication [5]. From X-ray diffraction and quantitative analysis by thermogravimetry of oxidizable cations [5], a cationic distribution of the type

$$(\mathrm{Mn}^{2+}_{0.8x}\mathrm{Zn}^{2+}_{y}\mathrm{Fe}^{3+}_{1-0.8x-y})_{\mathrm{A}}(\mathrm{Fe}^{3+}_{1+0.6x+y}\mathrm{Fe}^{2+}_{1-0.8x-y}\mathrm{Mn}^{3+}_{2x})_{\mathrm{B}}\mathrm{O}^{2-}_{4} \qquad (1)$$

can be proposed, where the subscripts A and B represent the tetrahedral and octahedral sites, respectively. The powders examined by microscopy showed a particle size of about 1 μm.

A second set of ferrites, with the composition approaching the x and y values of the end members, were obtained from thermal decomposition of mixed oxalates of iron and manganese $(\mathrm{Fe}_{1-x}\mathrm{Mn}_x)\mathrm{C_2O_4}\cdot 2\mathrm{H_2O}$ ($x \simeq 1/3$) and iron and zinc $(\mathrm{Fe}_{1-y}\mathrm{Zn}_y)\mathrm{C_2O_4}\cdot 2\mathrm{H_2O}$ ($y \simeq 1/3$) which leads, through adequate thermal treatment at low temperature (< 650 °C), to manganese and zinc ferrite. The details of the method of preparation have been discussed before [10, 11].

It should be borne in mind that the label "$\mathrm{MFe_2O_4}$" usually given to the spinel phase does in no sense imply the existence of a stoichiometric ferrite-type compound. For manganese ferrite the chemical formula $(\mathrm{Fe}_{2.04}\mathrm{Mn}_x)\mathrm{O}_4$ with $x = 0.96$ should be preferred to "$\mathrm{MnFe_2O_4}$", and for zinc ferrite prepared at 600 °C with a Zn content of 2 (27.40 and 26.80 wt % Zn) the phase composition varied with the firing temperature (Table I) because zinc ferrite shows a tendency to loss of zinc oxide in a vacuum [8]. X-ray crystallographic analysis shows that the samples contain only the spinel phase for $y < 1$, but a small amount of ZnO is present for $y = 1$. As a result of thermal treatment in a vacuum, the partial reduction of the Fe^{3+} ions leads to the development of divalent iron in the ferrite without rupturing the lattice configuration. For these samples prepared by coprecipitation of mixed oxalates, the crystallite sizes are about 50 nm. At this point it is instructive to note that these finely divided mixed oxides could also be oxidized to metastable defect phases of the same spinel structure (below 550 °C) [11].

The d.c. conductivity was measured by means of a two-probe method on compressed sintered pellets between two platinum electrodes as described in a previous paper [12] in which the parameters affecting the measurements are also discussed. In addition the electrical conductivity can be explained on the basis of the Verwey mechanism [13] involving electron exchange between ions of the same element which are present in more than one valence state and distributed randomly over crystallographically equivalent lattice sites. Depending upon the extent of substitution, a number of such ions may be produced during oxidation or at the firing temperature of Mn–Zn ferrites.

3. Results and discussion

3.1. Electrical conductivity of zinc ferrites

The effect of losing zinc during the firing in a vacuum can be seen in Figs 1 and 2. Fig. 1 shows the $\log\sigma$ against $1/T$ plots for various finely divided zinc ferrites near stoichiometry (the spinel is stoichiometric for 24.12 wt % Zn). It is to be noted that the conductivities measured for the samples with excess ZnO (curves e and f) were much lower than those measured for the samples with a deficiency of ZnO (curves a, b, c and d). The values of $\log\sigma$ at 100 °C are plotted in Fig. 2 (curve a) as a function of y. The data indicate that a small change in y near stoichiometry alters the conductivity by several orders of magnitude.

The activation energy E_σ calculated between 100 and 450 °C from $\log\sigma = f(1/T)$ curves versus y is reported in Fig. 2 (curve b). Near the composition $\mathrm{ZnFe_2O_4}$, E_σ increases in a stepwise fashion. For $y < 1$, the experimental values of E_σ increase slowly from 0.22 eV ($y = 0.963$) to 0.27 eV ($y = 0.995$) and for $\mathrm{ZnFe_2O_4}$ with ZnO excess the values increase strongly and are about 0.56 eV.

Moreover, whatever the composition, where the zinc ferrites are oxidized at low temperature (400 °C), the conductivity decreases significantly (Fig. 1, dashed lines) but the effects are similar and it is observed that the conductivities are practically independent of the initial composition. The principal conduction mechanism is associated with the presence of vacancies. It has been established that the structural formula of oxidized zinc spinels can be written as

$$[\mathrm{Zn}^{2+}_{8y/(9-y)}\mathrm{Fe}^{3+}_{8(3-y)/(9-y)}\square_{3(1-y)/(9-y)}]\mathrm{O}^{2-}_{4} \qquad (2)$$

where □ is the vacant lattice site located at the B sites. Therefore, if all the Fe^{2+} ions initially in the sample are converted to Fe^{3+} ions, the probability of hopping is affected and oxidized samples show less conductivity.

The change in conductivity and activation energy near the stoichiometry is thus primarily due to the conversion of Fe^{2+} to Fe^{3+} ions. At this stage, it should be noted that for zinc ferrites with iron excess, our results concerning the activation energy are in

TABLE I Chemical analysis of zinc ferrite near stoichiometry, $\mathrm{Zn}_y\mathrm{Fe}_{3-y}\mathrm{O}_4$

Firing temperature (°C)	Zn (wt %)	y	Chemical formula
600	27.40	1	$\mathrm{ZnFe_2O_4}$ + ZnO (0.57 wt %)
1000	27.20	1	$\mathrm{ZnFe_2O_4}$ + ZnO (0.20 wt %)
1100	27.00	0.995	$(\mathrm{Zn}^{2+}_{0.995}\mathrm{Fe}^{3+}_{0.05})_{\mathrm{A}}(\mathrm{Fe}^{2+}_{0.05}\mathrm{Fe}^{3+}_{1.995})_{\mathrm{B}}\mathrm{O}^{2-}_{4}$
600	26.80	0.988	$(\mathrm{Zn}^{2+}_{0.988}\mathrm{Fe}^{3+}_{0.012})_{\mathrm{A}}(\mathrm{Fe}^{2+}_{0.012}\mathrm{Fe}^{3+}_{1.988})_{\mathrm{B}}\mathrm{O}^{2-}_{4}$
1000	26.45	0.975	$(\mathrm{Zn}^{2+}_{0.975}\mathrm{Fe}^{3+}_{0.025})_{\mathrm{A}}(\mathrm{Fe}^{2+}_{0.025}\mathrm{Fe}^{3+}_{1.975})_{\mathrm{B}}\mathrm{O}^{2-}_{4}$
1100	26.12	0.963	$(\mathrm{Zn}^{2+}_{0.963}\mathrm{Fe}^{3+}_{0.037})_{\mathrm{A}}(\mathrm{Fe}^{2+}_{0.037}\mathrm{Fe}^{3+}_{1.963})_{\mathrm{B}}\mathrm{O}^{2-}_{4}$

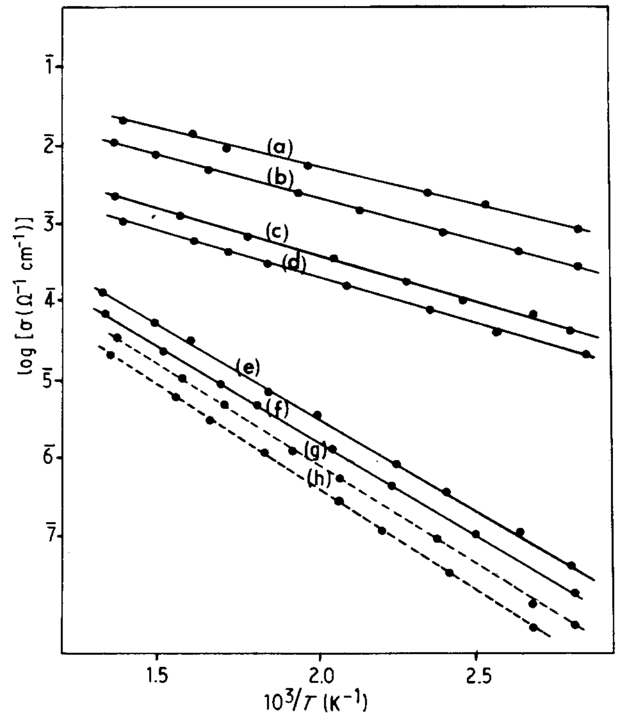

Figure 1 Conductivity of finely-divided zinc ferrites near stoichiometry, plotted on a logarithmic scale against reciprocal temperature for different Zn contents during the firing in vacuum: (a) $y = 0.963$, (b) $y = 0.975$, (c) $y = 0.988$, (d) $y = 0.995$, (e) $ZnFe_2O_4 + ZnO$ (0.20 wt %), (f) $ZnFe_2O_4 + ZnO$ (0.57 wt %). The dashed lines relate to oxidized spinel: (g) $y = 0.963$, (h) $ZnFe_2O_4 + ZnO$ (0.57 wt %).

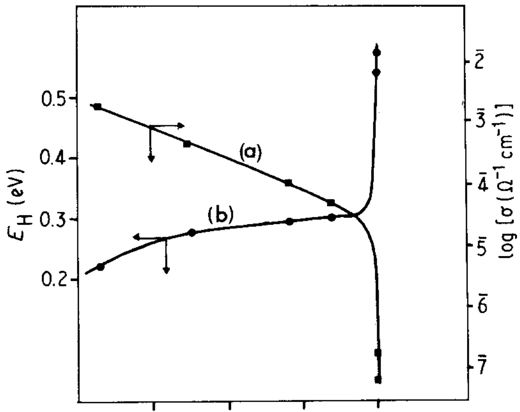

Figure 2 Compositional dependence of conductivity (curve a) and activation energy (curve b) for finely divided zinc ferrites.

approximate agreement with those reported by Rustamow *et al.* [14] (0.18 eV) and Prakash [15] (0.17 eV), suggesting for the ferrites prepared by these authors the presence of Fe^{2+} ions on B sites. By the extension of curve (b) of Fig. 2 toward lower E_σ values, we can estimate the Fe^{2+} content and propose for their zinc ferrites a composition close to $Fe_{2.046}Zn_{0.954}O_4$.

3.2. Electrical conductivity of Mn–Zn ferrites

As recalled in Section 1, the cation distribution in Mn–Zn ferrites can be structurally formulated as

$$(Mn^{2+}_{0.8x}Zn^{2+}_{y}Fe^{3+}_{1-0.8x-y})_A(Fe^{3+}_{1+0.6x+y}Fe^{2+}_{1-0.8x-y}Mn^{3+}_{0.2x})_B O^{2-}_4$$

where on the B sites Mn^{3+} ions occur, which are connected by the presence of Fe^{2+} ions on these sites.

Therefore, the electrical conductivity, which behaves according to the hopping process of electrons between Fe ions on the B sites, is given by a diffusion-type atomistic equation [16]:

$$\sigma = \frac{\text{Constant}}{T}\exp\left(-\frac{E_H}{RT}\right) \qquad (3)$$

where E_H is the activation energy of the conductivity process.

Log(σT) for the samples of $Mn_xZn_yFe_{2.044}O_4$ under vacuum (Fig. 3) and prepared by a ceramic route increases linearly with increase of temperature according to Equation 3, but for some samples the plot changes slope at the Curie temperature (T_c) (arrowed in Fig. 3). If the conductivity is mostly determined by the number of hopping processes, assuming the role of scattering phenomena and mean free path to be minimal, this change in slope indicates a change in the activation energy E_H. Therefore the process of hopping, although thermally activated in both regions, appears to have a lower E_H in the magnetic region below T_c. No Curie points are observed for the samples with $y = 0.70$ and $y = 0.956$, indicating the nature of these samples to be paramagnetic above room temperature. In Table II, values of T_c and E_H obtained from Fig. 3 are given.

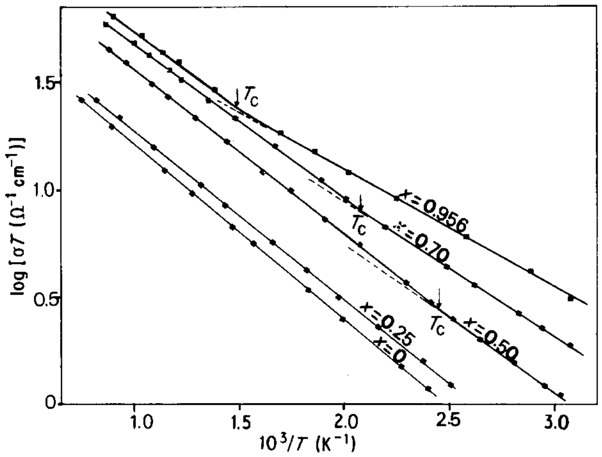

Figure 3 Plots of log(σT) versus $10^3/T$ for Mn–Zn ferrites. The Curie temperature is denoted by T_c.

TABLE II Values of Curie point T_c and activation energies E_H (for ferri- and paramagnetic regions) for Mn–Zn ferrites as a function of composition

y	T_c (°C)	E_H(ferri) (eV)	E_H(para) (eV)
0	400	0.124	0.204
0.256	230	0.152	0.189
0.50	125	0.167	0.182
0.70			0.177
0.956			0.172

It is seen that as the content of Zn increases, T_c decreases and E_H increases in the ferrimagnetic region, indicating that Zn^{2+} ions increase the resistance to hopping. This observation is in agreement with the results reported by Rezlescu *et al.* [17] and Satyanarajana *et al.* [18] who found that the conductivity of Li–Zn and Co–Zn ferrites decreases with increasing zinc content.

Concerning the Curie temperature for $MnFe_2O_4$ (673 K), intermediate values have been obtained by Mazen and Sabrah [19] (625 K) and by Yoo and Tuller [20] (700 K). These differences can be satisfactorily explained on the basis of a change of the $(Fe^{3+})/(Fe^{2+})$ ratio in B sites during the preparation of ferrite samples [19].

3.3. Behaviour of Mn–Zn ferrites in air

Fig. 4 shows the plots of log σ when samples of different compositions were heated in air at a constant rate of 2.5 °C min^{-1} from 100 to 700 °C. As already reported for manganese-substituted magnetites, several regions can be distinguished. In region I the conductivity strongly decreases with increase in temperature and as the concentration of Zn^{2+} ions is increasing the point A is moving toward higher temperatures from 270 °C for $x = 0.95$ to 435 °C for $x = 0$. This behaviour can be ascribed to the oxidation of Fe^{2+} ions and Mn^{3+} ions in B sites (Formula 1) and consequently to a decrease of Fe^{2+}–Fe^{3+} pairs with the formation of vacancies which minimize the conductivity. At this stage and whatever the position of point A, X-ray analysis should show a single phase of spinel structure with only a decrease of lattice parameter [5]. At higher temperatures than point A (region II), it is possible to see a broad maximum (dark zone) before or after the minimum (point M), particularly pronounced for manganese ferrite and missing for zinc ferrite.

The change that occurs in σ compared to the zinc ferrite can be regarded as being caused by the oxidation of Mn^{2+} ions into Mn^{3+} ions in A sites. However, as Mn^{3+} ions exhibit a strong tendency to octahedral coordination, the evolution of conductivity might not be associated with the hopping of electrons between Mn^{2+} and Mn^{3+} ions on A sites, but could be correlated with cation migration between the tetrahedral and octahedral sites of the spinel lattice. Thus, the conduction is likely to occur via hopping of electrons from lower-valent Mn^{3+} ions to higher-valent Mn^{4+} ions in B sites.

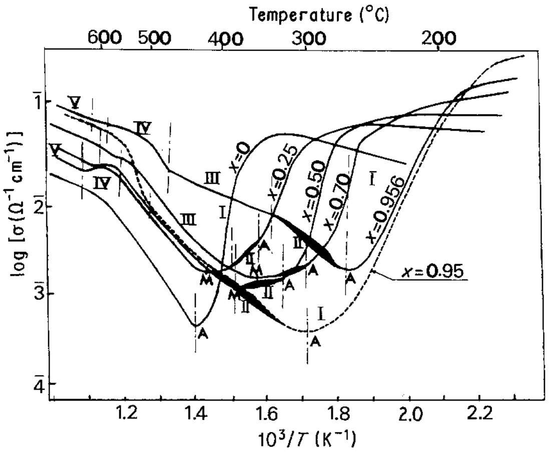

Figure 4 Behaviour of electrical conductivity in oxygen of Mn–Zn ferrites prepared by a ceramic route. The dashed line relates to a manganese ferrite prepared from mixed oxalate.

Beyond the dark zone, the $\log\sigma = f(T)$ curves show a non-linear conductivity in which two or three breaks (except for zinc ferrite) can be distinguished (regions III, IV and V). In the temperature range corresponding to region IV, the steep change in σ can be regarded as due to the oxidation of Mn^{2+} ions not completely oxidized at lower temperatures (region II) with the appearance of α-Fe_2O_3 accompanied by a cation-deficient spinel due to the presence of zinc, as confirmed by X-ray diffraction. However, in the case of manganese ferrite the cation-deficient spinel is converted into a rhombohedral phase α-$(Fe_{3-x}Mn_x)_{2/3}O_3$ from 600 °C. Moreover, the mass gain observed above 500 °C in the thermogravimetric curves further confirms the oxidation of Mn^{2+} ions during the phase change [5].

At higher temperatures, in region V, the percentage of α-Fe_2O_3 decreases whereas the lattice parameter is little influenced by the increase of temperature, which could be attributed to the beginning of the solubility of α-Fe_2O_3 in the spinel phase. Note, however, that for manganese ferrite the increase of temperature has an additional influence on the phases formed: the solubility of Mn_2O_3 in α-Fe_2O_3 decreases markedly and orthorhombic Mn_2O_3 is precipitated.

4. Conclusions

Concering the zinc ferrite spinel near stoichiometry, the general inferences that can be drawn from the above observations are as follows:

(a) Abrupt changes in conductivity and energy occur as the stoichiometry varies from an iron excess ($y < 1$) to a ZnO excess ($y = 1$).

(b) In iron-excess zinc ferrites the Fe^{2+} concentration in B sites is appreciable and in such cases the electrical conduction in this transition-metal oxide is believed to take place by electron hopping between Fe^{2+} and Fe^{3+} ions on two adjacent octahedral points in the spinel lattice. The high conductivity and the low value of the activation energy strongly indicate the presence of a small amount of Fe^{2+} ions in the lattice.

(c) In zinc ferrite with excess ZnO or in oxidized spinels in which the totality of iron cations are in the trivalent state, the probability of Fe^{2+} in the octahedral sites being very small or null, the electrical conduction is relatively poor.

For Mn–Zn ferrites the results reveal many interesting features:

(a) The introduction of Zn^{2+} ions in the lattice of $MnFe_2O_4$ results in a decrease in the ferrous ion content of B sites which is responsible for electrical conduction, thereby causing a decrease in the Curie temperature and in the bulk conduction. However, one may further conclude that the high electrical conductivities of Mn–Zn ferrites prepared by a ceramic route result from excess iron, a requirement for optimized magnetic properties.

(b) In the presence of oxygen, the electrical conductivity changes are in agreement with the relative availability for oxidation of Fe^{2+} and Mn^{2+} ions and with the distribution of cations between octahedral and tetrahedral sites. It has been shown that in the temperature range 100–600 °C, the oxidation temperature of each oxidizable cation increase with increase of Zn content. In the temperature range 100 to 450 °C, the Fe^{2+} ions at octahedral sites are oxidized preferentially, producing a large conductivity decrease due to the introduction of vacancies at B sites. Then, in the temperature range 300 to 550 °C, the Mn^{2+} ions at tetrahedral sites are partially oxidized, which favours electron exchange between manganese ions. Finally, at higher temperatures (> 600 °C) oxidation of the remaining Mn^{2+} ions is associated with a phase change which depends on the presence of zinc.

References

1. F. K. LOTGERING, *J. Phys. Chem. Solids* **25** (1963) 95.
2. B. GILLOT, M. EL GUENDOUZI, A. ROUSSET and P. TAILHADES, *J. Mater. Sci.* **21** (1986) 2926.
3. P. PERRIAT and M. ABOUAF, "Euro-Ceramics", Vol. 3 (Elsevier Applied Science, Amsterdam, 1989) p. 237.
4. P. PERRIAT, M. ABOUAF, D. BROUSSAUD and J. L. ROLAND, "Advances in Ferrites", Vol. 1 (ICFS, India, 1988) p. 75.
5. M. EL GUENDOUZI, K. SBAI, P. PERRIAT and B. GILLOT, *Mater. Chem. Phys.* **25** (1990) 429.
6. B. GILLOT and M. EL GUENDOUZI, *Thermochim. Acta* **162** (1990) 265.
7. L. G. Van ULTERT, *J. Chem. Phys.* **23** (1955) 1883.
8. K. KOUMOTO, H. YANAGIDA and S. MIZUTA, *J. Amer. Ceram. Soc.* **63** (1980) 17.
9. B. GILLOT and F. JEMMALI, *Phys. Status Solidi (a)* **76** (1983) 601.
10. B. GILLOT, R. M. BENLOUCIF and A. ROUSSET, *Mater. Res. Bull.* **16** (1981) 481.
11. B. GILLOT, M. EL GUENDOUZI, P. TAILHADES and A. ROUSSET, *React. Solids* **1** (1986) 139.
12. B. GILLOT and J. F. FERRIOT, *J. Phys. Chem. Solids* **37** (1976) 857.
13. B. GILLOT, M. EL GUENDOUZI and P. TAILHADES, *J. Mater. Sci.* **19** (1984) 3806.
14. A. G. RUSTAMOV, A. A. SAMOKHVALOV and I. G. FAKIDOV, *FTT* **5** (1963) 1031 (Soviet Physics–Solid State **5**, 751).
15. C. PRAKASH, *J. Mater. Sci. Lett.* **6** (1987) 651.
16. H. L. TULLER and A. S. NOWICK, *J. Phys. Chem. Solids* **38** (1977) 859.
17. N. REZLESCU, D. CONDURACHE, P. PETRARIU and E. LUCA, *J. Amer. Ceram. Soc.* **57** (1974) 40.
18. R. SATYANARAYANA, S. R. MURTHY and T. S. RAO, *J. Less-Common Metals* **79** (1981) 1.
19. S. A. MAZEN and B. A. SABRAH, *Thermochim. Acta* **105** (1986) 1.
20. H. I. YOO and H. L. TULLER, *J. Amer. Ceram. Soc.* **70** (1987) 388.

Received 20 April 1990
and accepted 15 January 1991